Cell, Vol. 80, 61–69, January 13, 1995, Copyright © 1995 by Cell Press

The Topology of the Kinetoplast DNA Network

Junghuei Chen,* Carol A. Rauch,†‡ James H. White,§ Paul T. Englund,† and Nicholas R. Cozzarelli*
*Department of Molecular and Cell Biology
University of California, Berkeley
Berkeley, California 94720
†Department of Biological Chemistry
Johns Hopkins University School of Medicine
Baltimore, Maryland 21205
§Department of Mathematics
University of California, Los Angeles
Los Angeles, California 90024

Summary

Kinetoplast DNA (kDNA) of trypanosomatid parasites is a network of ~5000 catenated DNA minicircles and ~25 maxicircles. We developed the following strategy to deduce the topological linkage of the minicircles of the Crithidia fasciculata network. First, we used graph theory to provide precise models of possible network structures. Second, on the basis of these models, we predicted the frequencies of minicircle oligomers expected from random network breakage. Third, we determined the fragmentation pattern of kDNA networks as a function of the extent of digestion. Fourth, by comparison of the results with the predictions, we identified the model that best represents the network. We conclude that each minicircle is linked on average to three other minicircles. A honeycomb arrangement probably results, with each minicircle typically at the vertex of a hexagonal cell. This topology has implications for the assembly, structure, and function of kDNA networks.

Introduction

Kinetoplast DNA (kDNA) is the mitochondrial DNA of trypanosomes and related protozoan parasites (for reviews, see Ray, 1987; Simpson, 1987; Ryan et al., 1988; Stuart and Feagin, 1992). The structure of kDNA is unique, consisting of a network of thousands of topologically interlocked circles. All of the DNA in the single mitochondrion of these organisms is organized into one kDNA network. Networks from the trypanosomatid Crithidia fasciculata, the subject of this report, are composed of about 25 maxicircles, 37 kb in size, and about 5000 minicircles, 2.5 kb in size. C. fasciculata differs from most other trypanosomatids in that its minicircles are nearly homogeneous, with more than 90% having the same nucleotide sequence (Sugisaki and Ray, 1987).

Like the mitochondrial DNAs of other eukaryotes, the maxicircles encode ribosomal RNAs and proteins involved in electron transport and oxidative phosphorylation (Simpson, 1987). The processing of the maxicircle transcripts, however, is highly unusual. Many transcripts undergo extensive editing, in which uridine residues are added or deleted at many specific sites to produce the translationally competent reading frame (reviewed by Simpson, 1990; Stuart and Feagin, 1992). Both the maxicircles and minicircles encode so-called guide RNAs, which, as complements of the edited transcripts, control the fidelity of the editing.

To understand the biological significance of the network, it is essential to learn more about its structure. As visualized by electron microscopy (EM), an isolated C. fasciculata kDNA network is an elliptically shaped two-dimensional array of DNA rings, about 10 μm by 15 μm in size (Pérez-Morga and Englund, 1993). However, the circles are much too crowded in the network for EM to reveal its underlying organization. We have already reported that the C. fasciculata minicircles are relaxed, unlike other circular DNAs in nature, which are negatively supercoiled. Furthermore, we found that minicircles within the network are catenated to other minicircles via a single interlock, an arrangement that provides strain-free connections (Rauch et al., 1993). Traditional structural methods are unable to reveal more about the topological connections within the network. We therefore developed a method that allows reconstitution of these connections from the structure and frequency of minicircle oligomers produced by partial restriction enzyme digestion. Using this method, we find that each minicircle in a nonreplicating C. fasciculata network is linked on average to three other minicircles, probably with each minicircle typically at the vertex of a hexagonal cell. We discuss the functional and evolutionary implications of this structural and topological arrangement.

Results

Solving the Network Structure: Theoretical Considerations

Simplifying Assumptions

A catenane of five minicircles is about the most complex catenane whose topology we can determine by the traditional methods of EM and gel electrophoresis. The kDNA network with thousands of linked rings is completely beyond these methods of analysis. In developing a method to determine the linkage pattern of kDNA, we made three major simplifying assumptions. First, we consider only the catenation of minicircles and neglect maxicircles. Second, we accept that the network is a monolayer. Third, we assume that each minicircle is linked identically to its neighbors. All three assumptions are supported by the available experimental data.

The first simplification, neglect of maxicircles, is justified by the fact that a C. fasciculata network has only about 25 maxicircles, compared with 5000 minicircles (Marini et al., 1980). Furthermore, selective removal of the maxicircles by PstI digestion leaves the network essentially unchanged as viewed by EM (D. Pérez-Morga and P. T. E.,

‡Present address: Department of Laboratory Medicine, Yale University School of Medicine, New Haven, Connecticut 06519.

unpublished data). Also, kDNA from Trypanosoma evansi, which is naturally deficient in maxicircles, is indistinguishable by EM from kDNA of the closely related parasite T. brucei, except for the absence of maxicircle loops (Hoeijmakers and Weijers, 1980).

The second assumption, that the network is a monolayer, is strongly supported by EM and by fluorescence microscopy of ethidium-stained networks. By either technique, the isolated network appears to be a flat or cup-shaped sheet of DNA. Even in the highly condensed state inside the parasite mitochondrion, the network is still basically a monolayer (Ferguson et al., 1992).

The third assumption, that of uniformity, is clearly a simplification of the actual structure. The three potential sources of heterogeneity in the network that are ignored are edges, holes, and hypercatenation. Rings at the boundaries of a network are expected to have fewer neighbors than internal rings, but these represent only a small fraction (about 4%) of the total rings. Network holes, interior areas where minicircles are missing or catenated to an incomplete complement of neighboring rings, are rarely observed by EM of C. fasciculata networks. Theoretical calculations show that a small number of randomly placed holes will not significantly alter our results. Hypercatenation, rings linked to more than the average number of rings, must be as rare as hypocatenation.

Strategy for Solving the Network Structure

Given these assumptions, we need only to determine two parameters to specify network topology uniquely: first, the number and arrangement of minicircles linked to each minicircle, and second, the topology of the linkage between catenated pairs of minicircles. The second parameter is adequately determined. Rings are exclusively singly linked to other rings (Rauch et al., 1993), and the relative orientation of any pair of rings is probably random.

Our strategy for determining the first parameter, the pattern of neighbors of each ring, contains the following steps: first, we model possible network topologies, using graph theory; second, we use the models to predict the nature of products from a random breakage of networks; third, we partially restrict kDNA networks and determine the relative amounts of each fragment type; fourth, we compare our results with the predictions and identify the model that most closely represents the kDNA network.

Modeling Network Structure Graphically

In graphic diagrams of model networks, a small circle, or vertex, represents a minicircle, and the line that connects vertices, or an edge, represents the topological linkage. Thus, O——O symbolizes a catenated minicircle dimer. Figure 1 shows graph diagrams of portions of the relevant model networks. The valence of a graph, *n*, is the number of edges incident to a vertex, or, equivalently, the number of rings linked to each ring. For the diagrams in Figure 1, *n* is equal to 3 in 1A–1D, 4 in 1E and 1F, and 6 in 1G. The concept of valence is analogous to its use in chemical bonding.

Every interior vertex in each diagram in Figure 1 has the same valence. At the boundaries of the diagram, however, the valence of a vertex is often less. In an infinite graph, there are no boundaries, and the valence is the same everywhere. We can model the kDNA network using univalent infinite graphs because of the large number of rings in the network.

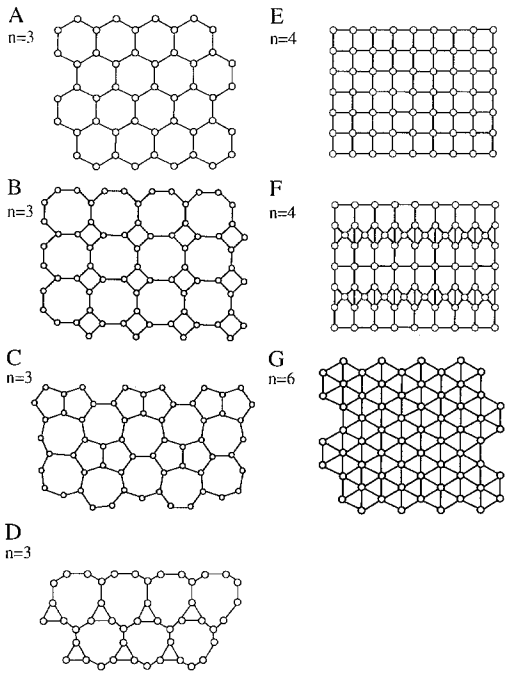

Figure 1. Models of Possible Connections in the kDNA Network

Shown are portions of infinite planar graphs that model portions of the possible topologies for the kDNA catenated network. The vertices of the graphs (small circles) represent the minicircles, and the edges (lines) the topological bonds between the circles. *n* is the valence of the graph. A tile is defined as the region of a planar graph bounded by edges. These are the only infinite planar graphs possible that are univalent and have either one tile or two equally represented tiles.

A planar graph is one that can be drawn without an edge crossing. The technical term planar is similar in meaning to the term two-dimensional in common usage. A rigorous statement of our second simplifying assumption is that the kDNA network can be represented by a planar graph. Because of the two-dimensionality of the kDNA network, all graphs considered in this paper are planar.

We define a tile as the region of a planar graph that is bounded by edges. Thus, the tiles in Figure 1A are hexagons, and those in Figure 1E are squares. All the tiles are the same for a regular graph, such as in Figures 1A, 1E, and 1G. A univalent graph need not be regular. Models A–D in Figure 1 all have valence 3, but only model A is regular. Models B–D are composed of equal numbers of two different tiles, as is model F. Figure 1 illustrates all possible infinite graphs that have equal numbers of two tiles or a regular tiling pattern.

Euler's theorem governs the relationship between the number of vertices (v), tiles (t), and edges (e) of a graph. It states that in an infinite graph:

$$v + t - e = 0$$

The importance of Euler's theorem for determining kDNA

Number of rings in fragment	Fragment structure	Network Model A	B	C	D	E	F	G
1	*	+	+	+	+	+	+	+
2	*	+	+	+	+	+	+	+
3	*	+	+	+	+	+	+	+
		-	-	-	+	-	+	+
4	*	+	+	+	+	+	+	+
	*	+	+	+	+	+	+	+
		-	-	-	+	-	+	+
		-	+	-	-	+	-	-
		-	-	-	-	-	+	+
5	*	+	+	+	+	+	+	+
		-	-	-	+	+	+	-
	*	+	+	+	+	+	+	+
		-	-	+	-	-	+	-
		-	+	-	-	+	-	-
		-	-	-	+	-	+	+
		-	-	-	+	-	+	+
		-	-	-	-	-	+	+
		-	-	-	-	-	+	+
		-	-	-	-	-	-	+

Figure 2. Fragments of Networks

Shown are graph diagrams for all possible arrangements of catenanes containing 1–5 rings that are subsets of infinite graphs of the indicated network models. The small circles represent minicircles, and the lines are the topological links between the minicircles. At the top, model networks are indicated by capital letters as in Figure 1. The vertical lines group models with the same valence: A–D (3); E–F (4); and G (6). Asterisk indicates the seven observed species, as described in the text.

structure is that it limits the valence (n) of an infinite graph such that

$$\langle E \rangle = \frac{2n}{n-2}$$

where $\langle E \rangle$ is the average number of edges per tile (see Rauch, 1991). Therefore, $\langle E \rangle$ is a function only of n and is independent of the tiling pattern.

A planar infinite network must have a valence no greater than 6. If n were greater than 6, then $\langle E \rangle$ would be less than 3. This is impossible, because the smallest plane tile is a triangle. To tile a plane without holes, n must be greater than or equal to 3. In fact, the valence can be only 3, 4, or 6 if the graph is regular or has two different tiles of the same number, the set to which we restrict ourselves. The simplification introduced by this treatment is substantial. Determining network structure started out as an intractable problem that could not be solved by any known method, but it is now reduced to determining whether the valence of the network is 3, 4, or 6 and deciding among the small number of tiling patterns shown in Figure 1.

Testing the Models

We fragmented kDNA into small catenanes (≤5 rings) whose structure we could determine and reconstructed the topology of the network from the relative abundance of such oligomeric catenanes. By modeling the kDNA network in terms of graphs, the fragmentation patterns can be predicted exactly.

We implemented this approach in two ways. First, we identified the topology of the network fragments and sought fragments that were either diagnostic of or incompatible with a particular model. For example, a network that contains a tile of n edges must yield a cyclic catenane fragment of n rings. We systematically enumerated all possible network fragments for the seven models in Figure 1. In Figure 2 are shown all the catenanes containing up to five linked rings that are consistent with these models.

The second way we implemented the method relies on the predictive power of the frequency of the abundant nondiagnostic fragments. Upon partial digestion, a circle has probability p of being linearized and q of surviving. Table 1 lists the probabilities of catenated fragments in terms of p and q for the seven model networks. For a circle to survive as a monomer, it must itself survive digestion, the probability of which is q, and all of its neighbors must be cut. Since n, the valence, is the number of neighbors of each circle, the probability of hitting all of the neighbors is p^n. Therefore, the number of circles that survive as monomers divided by the total number of circles is just qp^n (Table 1, row 1). The predicted surviving fraction of dimeric catenanes (Table 1, row 2) and of catenated linear trimers (Table 1, row 3) was derived similarly. The frequency of dimers and trimers is a function not only of valence but also of tiling pattern. Because the amounts of tetrameric and larger catenanes were too low to be measured accurately, we did not calculate their theoretical frequencies.

In Figure 3, the predicted frequency of surviving monomers, dimers, and trimers is plotted as a function of p, the probability of linearizing a circle, for all the model networks. These curves illustrate the predictive power of fragment frequencies and guided the choice of p that discriminates best among the models. The optimum strategy called for a p of between 0.3 and 0.7.

Solving the Network Structure: Experimental Considerations

Our experimental approach consisted of the following: random breakage of networks to various extents; fractionation of the products by gel electrophoresis; identification and quantitation of the species within each electrophoretic band; and comparison of the results with predictions from the model networks.

Random Breakage of Networks and the Pattern of Products

To disrupt networks partially, we used a restriction enzyme that cleaves each minicircle once. Ideally, every minicircle, whether catenated or free, should have an equal chance of being hit throughout the course of the reaction. This ideal may not be achieved, because the network might hinder restriction sterically or enhance digestion by providing a high local substrate concentration. We found that, up to about 35% digestion, the rate of attack by XhoI on monomer and network was the same (data not shown). Beyond that, monomers were digested up to twice as efficiently as network minicircles. We calculated that up to 50% digestion, the maximum error in minicircle valence introduced by nonrandom digestion was only 4% and therefore was ignored.

After partial digestion with XhoI, the fragments were resolved by high resolution agarose gel electrophoresis (Figure 4a). The pattern of oligomeric catenanes (Figure 4a,

Table 1. Predicted Frequencies of Monomer, Dimer, and Trimer Catenanes of Model Networks

Catenane	Model A (n = 3)	Model B (n = 3)	Model C (n = 3)	Model D (n = 3)	Model E (n = 4)	Model F (n = 4)	Model G (n = 6)
Monomer	qp^3	qp^3	qp^3	qp^3	qp^4	qp^4	qp^6
Dimer	$3q^2p^4$	$3q^2p^4$	$3q^2p^4$	$2p^3q^2(\frac{5}{6}p + \frac{2}{3})$	$4q^2p^6$	$2\frac{p^4q^2}{5}(2p^2 + 7p + 1)$	$6q^2p^8$
Trimer	$9q^3p^5$	$3q^3p^4(2p + 1)$	$6q^3p^5$	$p^3q^3(\frac{7}{3}p^2 + 4p + 2)$	$6q^3p^7(2 + p)$	$\frac{3p^5q^3}{5}(\frac{10}{3}p^3 + 12p^2 + \frac{22}{3}p + \frac{14}{3})$	$27q^3p^{10}$

The model networks are displayed in Figure 1, and n is the valence of the network. The calculated frequencies of catenanes are expressed in terms of p, the fraction of circles that are linearized, and q, the fraction of circles that survive digestion. The number of rings surviving as monomeric, dimeric, and trimeric catenanes are tabulated as a fraction of the total number of rings in the network. Cyclic trimeric catenanes will be produced only in models D, F, and G networks; their frequencies as a fraction of total trimeric catenanes are 6/25, 7/41, and 2/5, respectively.

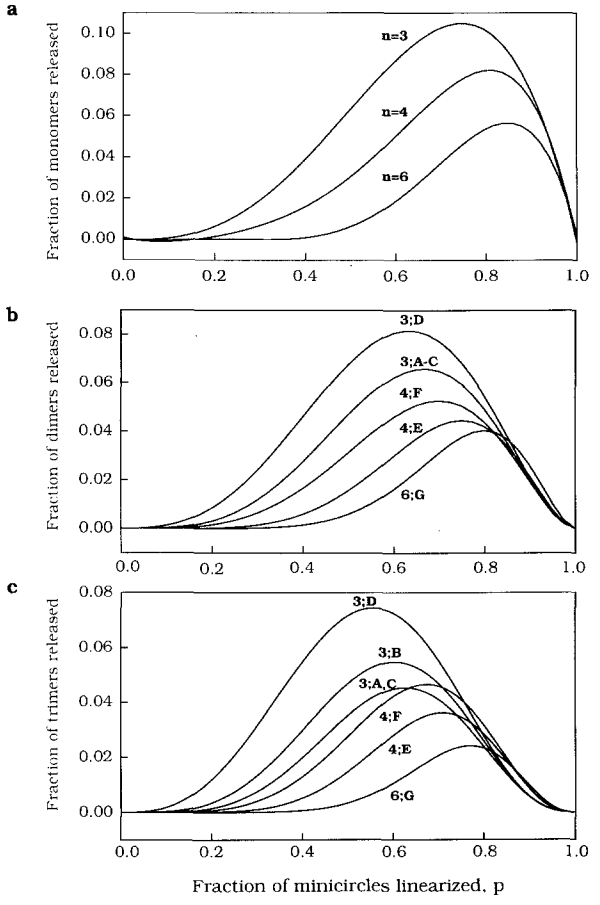

Figure 3. Predicted Frequencies of Fragments from Partial Digestion of Networks

The fractional survival of monomers (a), dimers (b), and linear catenated trimers (c) is plotted as a function of the fraction of circles restricted, p, for the model network. The models are indicated on the curves by their valence and their letter designation in Figure 1. Only valence is shown in (a), because the pattern of monomer release is independent of tiling.

lane 1) is similar to that produced by DNA gyrase catenation of minicircles (Figure 4a, lane 4). This similarity simplified identification of the bands and supports the view that the network is constructed stochastically by a type 2 topoisomerase. Digestion with excess XhoI confirms that virtually every minicircle is susceptible to cleavage (Figure 4a, lane 3).

In addition to linear monomers, we identified five major electrophoretic bands, labeled 1 through 5 (Figure 4a, lane 1), resulting from partial digestion. Band 1 is a minicircle monomer as shown by comigration with a standard (Figure 4a, lane 2). Band 2 was shown to consist of singly interlocked catenanes by EM of RecA-coated DNA (Figure 5A) and by comigration with a marker generated with DNA gyrase (Krasnow et al., 1983). Band 3 consists of linear trimers, as shown by EM (Figure 5B) and comigration with the gyrase standards. Band 4 contained linear and branched catenated tetramers that resolved after a longer electrophoretic run (data not shown). The faster-migrating species was shown by EM to be linear tetramers (Figure 5C), and the slower species was branched tetramers (Figure 5D). The longer electropheretic run showed that the ratio of these was 2:1. Band 5 was identified as catenated pentamers by EM (data not shown). Of the 14 pentamers analyzed, 6 were linear, and 8 were branched like isopentane:

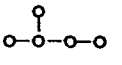

All the rings of the catenated oligomers (bands 2–5) were joined by a single interlock.

Thus, we have identified only 7 of the 20 possible fragments containing up to five rings (asterisk in Figure 2). The 13 missing fragments could either be incompatible with the structure of the kDNA network or be produced at an undetectable frequency. We believe that the absence of cyclic trimers is diagnostic of network structure. All 420 trimers that we could score unambiguously by EM were linear catenanes. We do not think that we missed cyclic trimers because of an unusual electrophoretic mobility. The trimer band analyzed by EM was from gels deliberately not run far enough to resolve the tetrameric and pentameric isomers. Moreover, we did not detect a band behind linear trimers, the expected position for cyclic trimers, even after long electrophoretic runs. The absence of cyclic trimeric fragments eliminates all models with triangular tiles: models D, F, and G in Figure 1. For all these models, a significant fraction of cyclic trimers is expected (see Table 1 legend).

We also never saw a pentamer branched like neopentane:

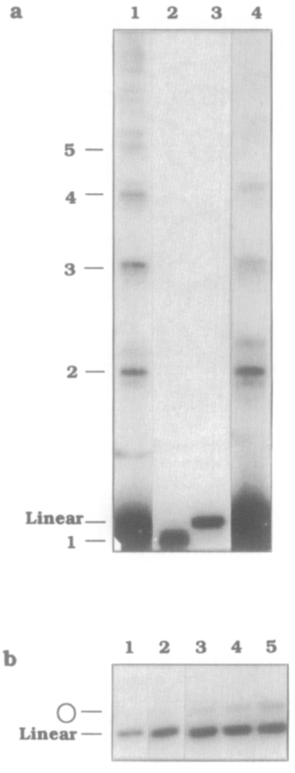

Figure 4. Resolution by Gel Electrophoresis of the Products Generated by Random Breakage of the kDNA Network by the XhoI Restriction Enzyme

After partial digestion of a kDNA network, the products were resolved by electrophoresis through high-resolution agarose gels (a) and TBE gels (b). The bands in (a) are labeled 1, 2, 3, 4, and 5 according to the number of constituent rings. Lane 1 contains the products of partial digestion, lane 2 has a monomer circular ring, lane 3 contains the products of complete digestion, and lane 4 is a marker of catenated minicircles generated by DNA gyrase. In (b), the network was digested for 5 min (lane 1), 10 min (lane 2), 20 min (lane 3), 30 min (lane 4), and 45 min (lane 5). The faster-migrating band is linear minicircle, and the slower-migrating band is monomer ring.

The significance of this absence is less certain, because we determined by microscopy the structure of only 14 pentamers, of which 6 were linear and 8 were isoforms. If the neopentane form is truly missing, it would rule out models E and F (see Figure 2). These models are also ruled out by the valence measurement discussed in the following section.

The only model that predicts only those seven fragments found is model A, the regular honeycomb pattern and the simplest model (see Figure 2). All the other models predict additional fragments.

Determination of Network Valence from the Frequency of Monomer, Dimer, and Trimer Fragments

We determined the valence of the kDNA network from three independent sets of data. We first measured with Tris–borate–EDTA (TBE) gels (e.g., Figure 4b) the fractional release of minicircle monomers and linearized minicircles as a function of the extent of XhoI digestion. Using the formula in the legend to Figure 6a, we then calculated the mean valence. Despite the scatter in the data, it is clear that the valence of the network is about 3 (Figure 6a). Of the 42 independent network fragmentations, the mean value of n was 2.96, and the standard deviation was 0.19.

We next measured by high resolution gel electrophoresis (e.g., Figure 4a) the release of catenated dimers. Figure 6b shows the fractional release of dimers as a function of the extent of network digestion with XhoI and the theoretical curves for dimer release from all the model networks. The 29 data points scatter about the theoretical curve for models with a valence of 3, models A–C. These three models are indistinguishable by this test. The data do not fit the theoretical curves for the models with a valence of 4 or 6 or for model D (valence 3).

The third experiment was the determination of the amount of linear trimeric catenanes by high resolution gel electrophoresis (e.g., Figure 4a) as a function of extent of XhoI digestion. The results are shown in Figure 6c, along with theoretical curves for all the models. Once again the data are consistent only with a network valence of 3, except perhaps for model F. Both dimeric and trimeric catenane generation can be a function of tiling pattern and not just valence, but the scatter in the data does not allow us to determine the tiling pattern.

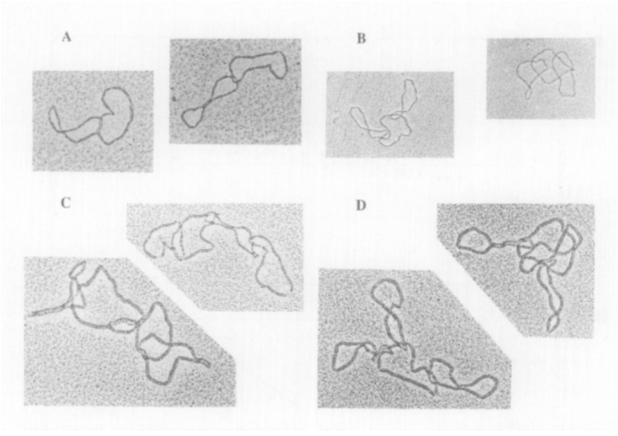

Figure 5. Identification of Network Fragments by Electron Microscopy

Bands from the electrophoresis of a partially degraded network (as shown in Figure 4a, lane 1) were excised from the gel, coated with RecA, and viewed by electron microscopy. Band 2 is a dimeric catenane (A). Band 3 is a linear trimeric catenane (B). Of 422 molecules scored by microscopy, 420 were clearly linear trimers. Band 4 consisted of linear (C) and branched (D) tetrameric catenanes. All the catenanes were joined by single interlocks.

Discussion

Topology of the C. fasciculata kDNA Network

We showed previously that the minicircles in the kDNA network are relaxed and singly interlocked to each other (Rauch et al., 1993). To determine the longer-range structure of the network, we needed to know the network valence and tiling pattern. In this paper, we showed that the

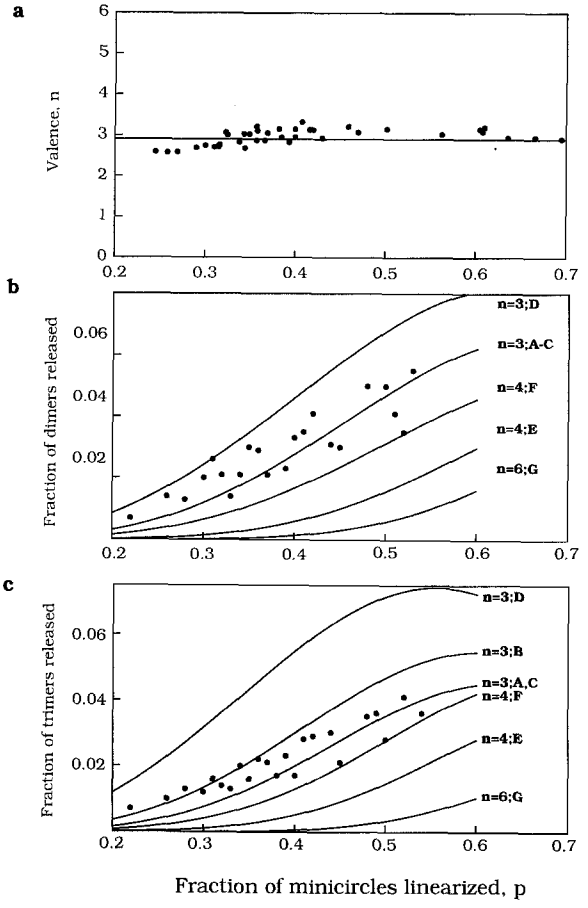

Figure 6. Frequencies of Fragments from Partial Digestion of Networks

(a) Determination of network valence from the fractional release of monomer circles. The kDNA network was partially digested to the extent shown, p. The plotted values of the valence, n, were computed from the relationship

$$n = \frac{\log(mon) - \log N - \log q}{\log p}$$

where *mon* is the number of monomer circles released, N is the total number of circles, and q is the surviving fraction of circles.

(b) The fraction of catenated dimers released as a function of partial digestion of kDNA networks. The amount of catenane dimers released as a function of linearization, p, of the network was measured by high resolution agarose gel electrophoresis. The theoretical curves for the model networks in Figure 1 are shown. The equations for the theoretical curves are in Table 1.

(c) The fraction of catenated trimers released as a function of network digestion. The theoretical curves are for the models in Figure 1. The equations for the curves are in Table 1.

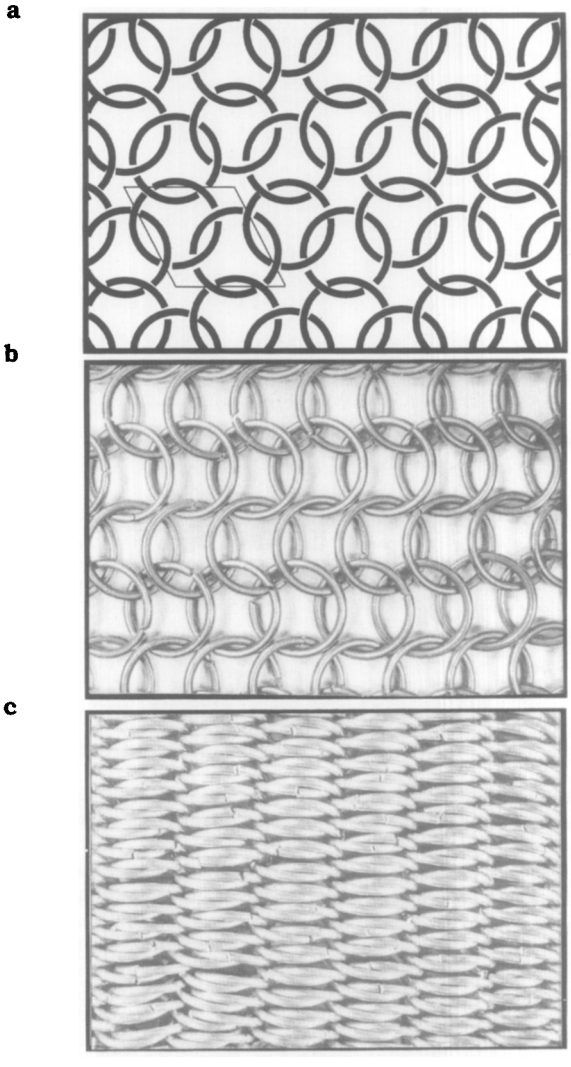

Figure 7. Models of the C. fasciculata kDNA Network

(a) Planar representation. Each circle represents a kDNA minicircle. The orientation of the rings imposed by base sequence is ignored, so that no sign is attached to the crossing of the rings. A rhomboid unit cell of the repeating pattern is shown at the lower left. The plane group is similar to p6, and each unit cell has a total of two rings and three topological bonds. There is a 6-fold rotation axis at each corner of the unit cell (the center of the hexagon of rings), two 3-fold axes in the interior of the cell (the center of each ring), and 2-fold axes on each edge and in the center of the unit cell (between each pair of rings). The diagram is scaled to the area of the isolated C. fasciculata network.

(b and c) Chain mail models for the C. fasciculata kDNA network, with a valence of 3.

(b) Model with the dimension of the isolated network. Each ring is 0.27 μm in diameter, and the total area of a network of 5000 rings is about 150 μm^2. Note the pleating of the network.

(c) Collapsed form of network, nearly of the size of the network in vivo. The rings touch within and between rows and are, on average, perpendicular to the plane of the network.

average valence is 3. The fragmentation pattern suggested that the tiling pattern is the hexagonal array shown in Figure 1A. It is the only pattern that predicts only the seven fragments found. This pattern is pleasing mathematically and physically. It is the only regular tiling pattern of valence 3 and is the simplest way to tile a plane. This tiling pattern is an energetically favorable one that is found throughout nature, for example, in the honeycombs of bees.

We adopt this topological arrangement for kDNA for the rest of the discussion, but we emphasize two limitations to our assignment. First, we have not proven model A, as opposed to another with valence 3. We feel confident only in excluding model D or any other model that involves significant use of triangular tiles. Definitive proof of model A requires EM identification of the topology of diagnostic

fragments that contain ≥6 rings or quantitation of the release of fragments with ≥4 rings, and both of these experiments are beyond current methodology. Second, we measured only the mean valence and do not know the deviation from the mean. Thus, there could be some rings with valence 2 and others with 4, averaging to 3. Because EM of C. fasciculata networks reveals a fairly uniform structure, with few holes, we think that the variation from 3 cannot be too great.

Structure of the C. fasciculata kDNA Network

The topological diagram of the kDNA network that we have deduced immediately suggests a physical structure. We first depict the network structure in a simplified planar diagram, so that the underlying organization is easy to see (Figure 7a). Each minicircle is represented by a perfect circle. The plane group of the lattice is similar to p6, a group with high symmetry. The unit cell contains a catenated dimer of minicircles (Figure 7). Thus, the network pattern can be built up very readily from a simple unit cell.

The packing of the DNA into the network can be better appreciated by constructing a three-dimensional model. A convenient material is chain mail, such as was used in medieval armor. The individual rings of the mail are the minicircles. Chain mail with the topology of C. fasciculata kDNA is shown in Figures 7b and 7c. The model in Figure 7b has the packing density of an isolated protein-free kDNA network. The model in Figure 7c has nearly the density of the network in vivo. Several features are evident from a consideration of the chain mail models.

First, both chain mail networks are surprisingly flexible and readily lie on a flat surface. No major steric problems are imposed by the linking pattern. This helps explain why the linkage of 5000 DNA rings in the kDNA network does not strain the individual rings at all (Rauch et al., 1993).

Second, an orderly close packing of the rings is achieved by a pleating of the mail. The mail is organized into rows of rings that tilt in the same direction, and an alternation of tilt direction between rows generates the pleats. While the 2.5 kb DNA minicircle is obviously more flexible than a steel ring, the minimum enthalpy conformation of an isolated kDNA network is probably a fairly regular one analogous to that depicted in Figure 7b. The pleating of the network allows two rings to pack into a unit cell of about the size of a single ring, 0.27 μm in diameter. The C. fasciculata network in vitro has an area of about 150 μm^2. Since there are 5000 rings in the network, the unit cell side is 0.25 μm long.

Third, the model network can readily be contracted by stacking the rings, on average, perpendicular to the plane of the network (Figure 7c). This condensed form mimics the form of networks in cells. A comparison of electron micrographs of isolated networks and confocal fluorescence images of networks in situ implies that compaction in vivo is accomplished by shrinking of the distance between rings without folding the sheet and that the rings are aligned nearly perpendicular to the plane of the sheet (Ferguson et al., 1992). The area of the condensed chain mail network model is 2.7 μm^2. The rings of the actual network of DNA could easily deform and interpenetrate to get the additional compaction needed to match the dimensions found in vivo (0.8 μm^2).

Our conclusion is that our postulated network structure is compatible with all available data. Despite its apparent complexity, it is built up from a simple unit cell in a regular and symmetric fashion. The network is strain free in both the extended form found in vitro and the condensed form in cells.

Why Does a C. fasciculata Minicircle Have a Valence of 3?

A topoisomerase should form a catenated network from relaxed minicircles constrained in a plane at high concentration. A high DNA concentration entropically favors catenation, because catenation makes new configurations available. Counteracting this force is the increase of steric hindrance and electrostatic repulsion between DNA rings as the number of linked rings increases. It is likely that the minicircle valence reflects the equilibrium balance of these forces.

A C. fasciculata kDNA network in vivo is condensed into a disk roughly 1 μm in diameter and 0.4 μm thick (Ferguson et al., 1992). The perimeter of the disk may be limited by the mitochondrial inner membrane. Electron micrographs of thin sections of C. fasciculata and other trypanosomatids reveal that the kinetoplast disk usually directly abuts this membrane (e.g., Renger and Wolstenholme, 1972). The membrane may also confer the characteristic shape to the network. We propose that catenation of 5000 minicircles, constrained within this 1 μm by 0.4 μm disk, results in an average valence of 3.

When the network undergoes replication, minicircles are released from the network by topoisomerase action. After replication of the free minicircles, the progeny reattach to the periphery of the network (Ferguson et al., 1994; Pérez-Morga and Englund, 1993). Therefore, as minicircles are added to the incomplete valence shell at the network edge, the disk grows in size. Holes that develop in the center of the network, owing to minicircle release, are at least partially repaired by catenation of neighboring minicircles.

If there were more minicircles in the disk, the valence would be greater than 3. We find that this is the case for minicircles in a C. fasciculata network undergoing replication (J. C., P. T. E., and N. R. C., unpublished data). This higher valence may result from the doubling of the number of minicircles during replication without a concomitant increase in the space occupied by the network. When the duplication of space as well as DNA is complete, the network valence returns to 3.

In the case of Leishmania tarentolae, where the minicircles are much smaller, isolated networks appear by EM to be irregular and full of holes. They are so fragile that they are difficult to isolate intact, and the network fragments contain linear chains of minicircles (P. T. E., unpublished data; Simpson and da Silva, 1971; Simpson and Berliner, 1974). Therefore, the average minicircle valence in L. tarentolae networks may well be less than 3.

A valence of 3 is an excellent choice for a highly concentrated array of rings that are constrained into a plane. Lin-

ear arrays of catenated rings, with or without branching, have a valence close to 2. A valence of 3 is the lowest value that will give a regular network that fills a plane. A valence of 4 or more is readily compatible with three-dimensional lattices, but the kDNA network is a two-dimensional lattice.

Not only must minicircles be packed at high concentration to form a network, but it is essential that they be relaxed. This has been demonstrated by in vitro experiments. In the presence of a DNA-aggregating agent such as spermidine, DNA gyrase forms a network of thousands of relaxed ColE1 rings (Kreuzer and Cozzarelli, 1980). Under the same conditions, gyrase formed only small oligomers of supercoiled ColE1 DNA. We have found the same results with C. fasciculata minicircles (unpublished data). The reduced space in the interior of a supercoiled molecule decreases the equilibrium constant for catenation by orders of magnitude (A. Vologodskii and N. R. C., unpublished data). This explains why minicircles of the C. fasciculata network are relaxed, in contrast with all other DNAs in nature.

Why Is kDNA a Network?

The kDNA network is the mitochondrial chromosome of the trypanosomatid. The kDNA sequences are not organized into extremely long molecules as in nuclear chromatin; rather, they are in small- and moderate-sized rings that are linked topologically. In both networks and nuclear chromosomes, the DNA is compacted in part by a topological constraint, but the constraints are very different. In chromatin, DNA supercoiling is stabilized by a linking number deficit. In the kDNA network, the rings are compacted by catenation. In chromatin, compaction and organization are strongly affected by DNA binding to histones. Histones are not associated with kDNA (Borst and Hoeijmakers, 1979), but presumably other proteins help compact the network. The total compaction of nuclear and kinetoplast chromosomes is similar, about four orders of magnitude.

Supercoiling provides energy for DNA double helix unwinding and thereby facilitates processes such as replication and transcription. Why have trypanosomatids sacrificed minicircle supercoiling so that they can form a network? Some of the most ancient kinetoplastid protozoa do not have networks. In Bodo caudatus, the kDNA circles are not catenated (Hajduk et al., 1986), and in Trypanoplasma borreli the minicircle-like sequences are tandemly repeated on linear molecules (L. Simpson, personal communication). Since more recently evolved trypanosomes have networks, there is presumably some advantage to the network structure. One possibility is that catenation facilitates the interaction between maxicircle transcripts and minicircle-encoded guide RNAs. Another possible advantage of a network is that its structure permits rapid change in minicircle repertoire. Variation in minicircle content in different parasite isolates is well established (Borst et al., 1980; Morel et al., 1980; Wirth and Pratt, 1982). Minicircle exchange occurs during mating of T. brucei, as progeny parasites derive minicircles from both parents (Gibson and Garside, 1990).

A mutation in an edited region of a maxicircle could be lethal without a corresponding change in the minicircle encoding the guide RNA. Two simultaneous complementing mutations would be rare, but a constant influx of new minicircles during mating might increase the chance that one would provide the proper guide RNA for the mutated maxicircle sequence. Rapid variation of the guide RNA repertoire could be accomplished much more efficiently by exchanging minicircles between networks than by recombining genes on a linear chromosome. By this argument, the minicircles could be monomeric, but the clear advantage of a network is that it provides an orderly mechanism of replication and segregation of all the genetic information contained in the kDNA genome.

Experimental Procedures

Isolation of kDNA

C. fasciculata were grown to stationary phase (1×10^8 to 2×10^8 cells/ml) at room temperature in brain heart infusion medium supplemented with 20 μg/ml hemin. kDNA was isolated as described (Hajduk et al., 1984), except that the sarkosyl lysate was digested with RNase A (200 U/ml) and RNase T1 (0.2 mg/ml) for 90 min at 37°C prior to centrifugation in a CsCl step gradient.

Enzymes

Restriction endonuclease XhoI was from Boeringer Mannheim Biochemicals. Escherichia coli DNA gyrase subunits A and B were purified by minor modifications of published procedures (Mizuuchi et al., 1984).

Enzyme Reactions

To digest kDNA partially, 40 μl mixtures containing 50 mM Tris–HCl (pH 7.9), 10 mM $MgCl_2$, 100 mM NaCl, 1 mM dithiothreitol, 1 μg of kDNA, and 10 U of XhoI were incubated at 37°C for times ranging from 10 to 90 min. After heating to 70°C for 10 min, the DNA was nicked with 5–10 μg/ml DNase I in the presence of 300 μg/ml ethidium bromide for 30 min. The dye was removed by extraction with butanol and ether, and the DNA was precipitated with ethanol and resuspended in electrophoresis buffer.

For the decatenation of the kDNA network by T2 topoisomerase, the mixture (20 μl) contained 40 mM Tris–HCl (pH 7.8), 60 mM KCl, 10 mM $MgCl_2$, 0.5 mM dithiothreitol, 0.5 mM EDTA, 30 μg/ml bovine serum albumin, 0.5 mM ATP, 0.4 μg of kDNA, and 0.2 μg of T2 topoisomerase. Incubation was at 30°C for 1–6 hr.

Catenation of minicircles by DNA gyrase was at 30°C for 6 hr, and the reaction mixtures (0.3 ml) contained 15 mM Tris–HCl (pH 7.6), 20 mM KCl, 10 mM $MgCl_2$, 1 mM dithiothreitol, 1 mM ATP, 50 μg/ml albumin, 5 mM spermidine–HCl, 4 μg of purified minicircles, and 40 fmol of subunits A and B of gyrase.

Fractionation of Network Fragments by Gel Electrophoresis

Two electrophoresis systems were used. For optimal fractionation of catenated oligomers, digests were separated by high-resolution electrophoresis through a 0.8% agarose gel in 80 mM Tris–HCl (pH 7.5), 5 mM sodium acetate, 1 mM EDTA, and 0.03% SDS (Sundin and Varshavsky, 1980). The DNA was nicked with DNase I before fractionation to compact each catenane type into a single band. For optimum resolution of monomer minicircles from linearized minicircles, electrophoresis was through 0.8% agarose gels containing 90 mM Tris–HCl (pH 8.3), 90 mM sodium borate, and 2.5 mM EDTA (TBE). After electrophoresis, the gels were stained with ethidium bromide and photographed under UV light. The negatives of the films were analyzed by densitometry using a Hoefer GS 300 densitometer.

Electron Microscopy

Electron microscopy was used to identify the oligomeric kDNA fragments after electroelution from agarose gels. To visualize strand overlaps, the DNA was coated with RecA protein before viewing. Coating was done as described in Krasnow et al. (1983) or as in Thresher and Griffith (1990). The filtration column eluate from either method was applied to freshly glow-discharged precoated carbon–formvar grids

(Williams, 1977). The grids were rinsed seven times with 0.1 M ammonium acetate, stained in 5% uranyl acetate for 15 s, and rinsed seven times with 0.01 M ammonium acetate. Buffer was removed by suction. The grids were air dried, shadowed with Pt/Pd alloy (80%/20%) at an angle of 7°, and viewed in a JEOL100B electron microscope.

Acknowledgments

We thank Sylvia Spengler for her advice and encouragement throughout the project, and Hal Heydt of the Society for Creative Anachronism for the construction of the chain mail models of the kDNA networks. This work was supported by grants from the National Institutes of Health (GM31657) and the National Institute of Environmental Health Sciences (ES01896-15) to N. R. C., from the MacArthur Foundation and National Institutes of Health (GM27608) to P. T. E., and from the National Science Foundation (DMS-8820208) to J. W. and N. R. C.; C. A. R. was supported by Medical Scientist Training Grant 5T32GM07309.

Received August 11, 1994; revised October 11, 1994.

References

Borst, P., and Hoeijmakers, J. H. (1979). Kinetoplast DNA. Plasmid *2*, 20–40.

Borst, P., Fase Fowler, F., Hoeijmakers, J. H., and Frasch, A. C. (1980). Variations in maxi-circle and mini-circle sequences in kinetoplast DNAs from different *Trypanosoma brucei* strains. Biochim. Biophys. Acta *610*, 197–210.

Ferguson, M., Torri, A. F., Ward, D. C., and Englund, P. T. (1992). In situ hybridization to the *Crithidia fasciculata* kinetoplast reveals two antipodal sites involved in kinetoplast DNA replication. Cell *70*, 621–629.

Ferguson, M. F., Torri, A. F., Pérez-Morga, D., Ward, D. C., and Englund, P. T. (1994). Kinetoplast DNA replication: mechanistic differences between *Trypanosoma brucei* and *Crithidia fasciculata*. J. Cell. Biol. *126*, 631–639.

Gibson, W., and Garside, L. (1990). Kinetoplast DNA minicircles are inherited from both parents in genetic hybrids of *Trypanosoma brucei*. Mol. Biochem. Parasitol. *42*, 45–54.

Hajduk, S. L., Klein, V. A., and Englund, P. T. (1984). Replication of kinetoplast DNA maxicircles. Cell *36*, 483–492.

Hajduk, S. L., Siqueira, A. M., and Vickerman, K. (1986). Kinetoplast DNA of *Bodo caudatus*: a non-catenated structure. Mol. Cell. Biol. *6*, 4372–4378.

Hoeijmakers, J. H., and Weijers, P. J. (1980). The segregation of kinetoplast DNA networks in *Trypanosoma brucei*. Plasmid *4*, 97–116.

Krasnow, M. A., Stasiak, A., Spengler, S. J., Dean, F., Koller, T., and Cozzarelli, N. R. (1983). Determination of the absolute handedness of knots and catenanes of DNA. Nature *304*, 559–560.

Kreuzer, K. N., and Cozzarelli, N. R. (1980). Formation and resolution of DNA catenanes by DNA gyrase. Cell *20*, 245–254.

Marini, J. C., Miller, K. G., and Englund, P. T. (1980). Decatenation of kinetoplast DNA by topoisomerases. J. Biol. Chem. *255*, 4976–4979.

Mizuuchi, K., Mizuuchi, M., O'Dea, M. H., and Gellert, M. (1984). Cloning and simplified purification of *Escherichia coli* DNA gyrase A and B proteins. J. Biol. Chem. *259*, 9199–9201.

Morel, C., Chiari, E., Camargo, E. P., Mattei, D. M., Romanha, A. J., and Simpson, L. (1980). Strains and clones of *Trypanosoma cruzi* can be characterized by pattern of restriction endonuclease products of kinetoplast DNA minicircles. Proc. Natl. Acad. Sci. USA *77*, 6810–6814.

Pérez-Morga, D., and Englund, P. T. (1993). The structure of replicating kinetoplast DNA networks. J. Cell Biol. *123*, 1069–1079.

Rauch, C. A. (1991). The topology of kinetoplast DNA networks. PhD thesis, Johns Hopkins University, Baltimore, Maryland.

Rauch, C. A., Pérez-Morga, D., Cozzarelli, N. R., and Englund, P. T. (1993). The absence of supercoiling in kinetoplast DNA minicircles. EMBO J. *12*, 403–411.

Ray, D. S. (1987). Kinetoplast DNA minicircles: high-copy-number mitochondrial plasmids. Plasmid *17*, 177–190.

Renger, H. C., and Wolstenholme, D. R. (1972). The form and structure of kinetoplast DNA of *Crithidia*. J. Cell Biol. *54*, 346–364.

Ryan, K. A., Shapiro, T. A., Rauch, C. A., and Englund, P. T. (1988). The replication of kinetoplast DNA in trypanosomes. Annu. Rev. Microbiol. *42*, 339–358.

Simpson, L. (1987). The mitochondrial genome of kinetoplastid protozoa: genomic organization, transcription, replication, and evolution. Annu. Rev. Microbiol. *41*, 363–382.

Simpson, L. (1990). RNA editing: a novel genetic phenomenon? Science *250*, 512–513.

Simpson, L., and Berliner, J. (1974). Isolation of the kinetoplast DNA of *Leishmania tarentolae* in the form of a network. J. Protozool. *21*, 382–393.

Simpson, L., and da Silva, A. (1971). Isolation and characterization of kinetoplast DNA from *Leishmania tarentolae*. J. Mol. Biol. *56*, 443–473.

Stuart, K., and Feagin, J. E. (1992). Mitochondrial DNA of kinetoplastids. Int. Rev. Cytol. *141*, 65–88.

Sugisaki, H., and Ray, D. S. (1987). DNA sequence of *Crithidia fasciculata* kinetoplast minicircles. Mol. Biochem. Parasitol. *23*, 253–263.

Sundin, O., and Varshavsky, A. (1980). Terminal stages of SV40 DNA replication proceed via multiply intertwined catenated dimers. Cell *21*, 103–114.

Thresher, R. J., and Griffith, J. D. (1990). Intercalators promote the binding of RecA protein to double-stranded DNA. Proc. Natl. Acad. Sci. USA *87*, 5056–5060.

Williams, R. C. (1977). Use of polylysine for adsorption of nucleic acids and enzymes to electron microscope specimen films. Proc. Natl. Acad. Sci. USA *74*, 2311–2315.

Wirth, D. F., and Pratt, D. M. (1982). Rapid identification of *Leishmania* species by specific hybridization of kinetoplast DNA in cutaneous lesions. Proc. Natl. Acad. Sci. USA *79*, 6999–7003.